

IL NUOVO CIMENTO
DOI 10.1393/ncc/i2014-11754-x

VOL. 37 C, N. 2

Marzo-Aprile 2014

COLLOQUIA: LC13

Overview of ALICE results

M. GAGLIARDI

Università di Torino and INFN, Sezione di Torino - Torino, Italy

ricevuto il 4 Febbraio 2014

Summary. — The ALICE experiment at the CERN LHC studies the hot and dense medium formed in ultra-relativistic heavy-ion collisions, and the transition to Quark Gluon Plasma. Several observables are used to characterise the medium. In this contribution we report on the main ALICE results on global properties, particle spectra, anisotropies, heavy flavour and quarkonium production, obtained in Pb-Pb collisions at $\sqrt{s_{NN}} = 2.76$ TeV. Measurements performed in p-Pb and pp collisions are also part of the ALICE physics program: selected highlights from such measurements are discussed.

PACS 25.75.-q – Relativistic heavy-ion collisions.

PACS 12.38.Mh – Quark-gluon plasma.

PACS 47.70.-n – Reactive and radiative flows.

PACS 14.40.Pq – Heavy quarkonia.

1. – Introduction

The ALICE [1] experiment at the Large Hadron Collider (LHC [2]) was designed to study matter in ultra-relativistic heavy-ion collisions, at energy densities much larger than that of ordinary nuclear matter. Under these conditions, finite temperature QCD calculations on the lattice (see, *e.g.*, [3]) predict a transition to a deconfined state of matter known as Quark-Gluon Plasma (QGP). Measurements in proton-proton and proton-nucleus collisions are also crucial to the ALICE physics program, both as a reference for the interpretation of heavy-ion data and as a tool to probe QCD in previously unexplored domains. ALICE consists of a central barrel, covering the pseudo-rapidity range $|\eta| < 0.9$, where particles of transverse momentum p_T as low as 100 MeV/ c are tracked and identified, and a muon spectrometer ($-4 < \eta < -2.5$) for the detection of quarkonia and open heavy flavour at forward rapidity. In the first three years of LHC operation, ALICE took data in Pb-Pb collisions at $\sqrt{s_{NN}} = 2.76$ TeV, in p-Pb collisions at $\sqrt{s_{NN}} = 5.02$ TeV and in pp collisions at $\sqrt{s} = 2.76, 7$ and 8 TeV.

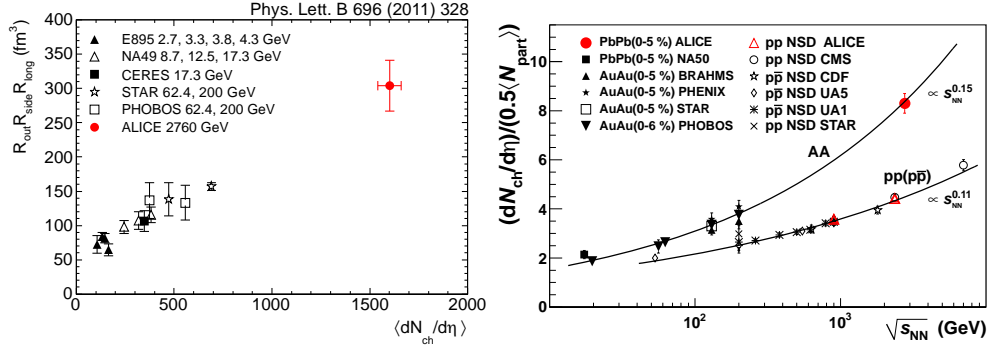


Fig. 1. – Left: product of the three fireball radii in Pb-Pb collisions, compared to lower energy measurements. Right: charged particle pseudorapidity density per participant nucleon in 0–5% Pb-Pb collisions, compared to measurements at different energies and colliding systems.

2. – Selected Pb-Pb results

The global properties of Pb-Pb collisions can be determined via Hanbury-Brown-Twiss interferometry of identical charged pions: the volume of the interacting fireball ($\simeq 300 \text{ fm}^3$) was found to be twice the value measured at top RHIC energy (fig. 1, left), and the lifetime ($\simeq 10 \text{ fm}/c$) about 20% larger [4]. The average charged particle density at mid-rapidity per participant nucleon was also measured [5], and found to be twice the value measured at RHIC (fig. 1, right). A preliminary measurement of the direct photon spectrum in 0–40% most central collisions yields a temperature of $304 \pm 51 \text{ MeV}$, which is about 40% larger than the one found at RHIC.

Identified particle spectra measured at low- p_T in central Pb-Pb collisions [6] have been described by a superposition of collective motion and thermal motion: blast-wave fits [7] indicate a radial flow velocity $\langle \beta \rangle = 0.65$ (10% larger than at RHIC) and a kinetic freeze-out temperature of about 95 MeV. The nuclear modification factors for (anti-)protons, charged pions and kaons were measured up to $p_T = 20 \text{ GeV}/c$ (fig. 2, left), and found to be all compatible above 7 GeV/c, suggesting that the medium does not affect the fragmentation strongly. In non-central Pb-Pb collisions, the initial spatial anisotropy of the collisions is converted into momentum anisotropy by the large pressure gradients, an effect

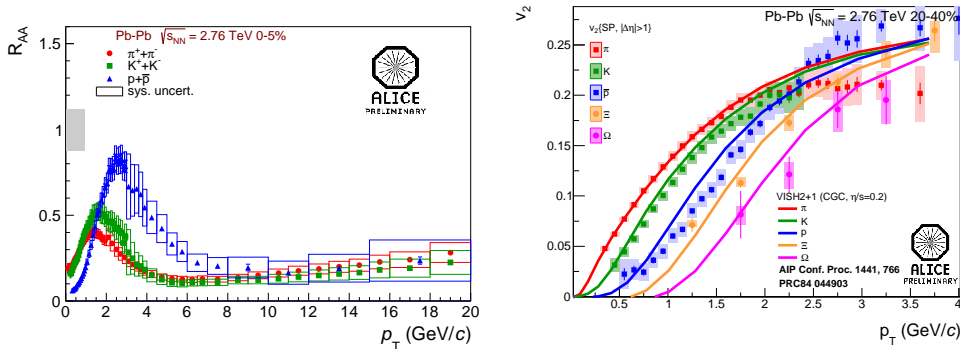


Fig. 2. – Left: nuclear modification factor $vs.$ p_T for pions, kaons and protons in Pb-Pb collisions. Right: v_2 $vs.$ p_T for identified particles in Pb-Pb collisions.

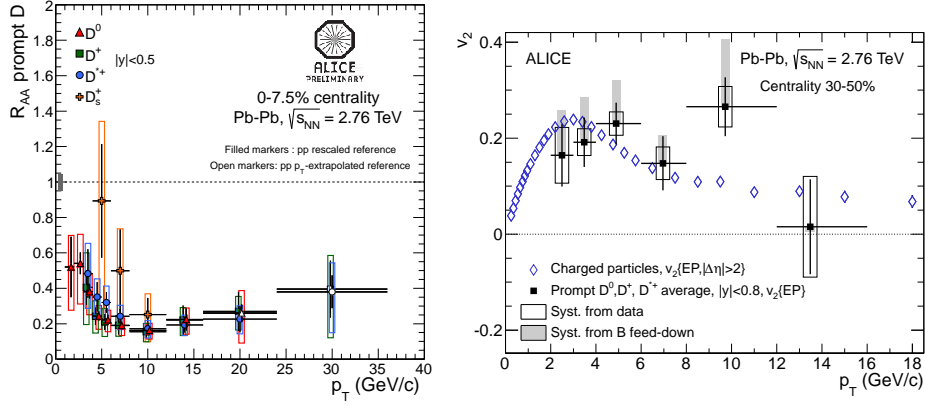


Fig. 3. – Left: nuclear modification factor as a function of p_T for prompt D^0 , D^+ , D^{*+} and D_s^+ mesons at central rapidity. Right: average of D^0 , D^+ , D^{*+} v_2 as a function of p_T , compared to charged-particle v_2 [10], measured with the event plane (EP) method.

quantified by the second Fourier component, v_2 , of the angular distribution of charged particles, which was measured as a function of transverse momentum for non-identified particles [8]. The measurement was recently extended to identified particles (fig. 2, right), with v_2 for 20–40% Pb-Pb collisions showing mass ordering up to and including multi-strange baryons. This behaviour is described by hydrodynamical models [9].

Heavy flavour particles (charm and beauty hadrons) are an important tool for probing the properties of QGP. They are sensitive to the medium density, through the mechanism of in-medium parton energy loss, which causes modifications of the momentum distributions in Pb-Pb collisions with respect to those in pp. The nuclear modification factor R_{AA} of D mesons is shown in fig. 3, left. Suppression by a factor up to 5 for $p_T > 5$ GeV/c is observed. The magnitude and pattern of suppression are similar for the three D meson species. Figure 3, right shows the measured v_2 of D mesons: it is similar in magnitude to that of charged hadrons [10], suggesting that charm quarks take part in the collective expansion of the medium.

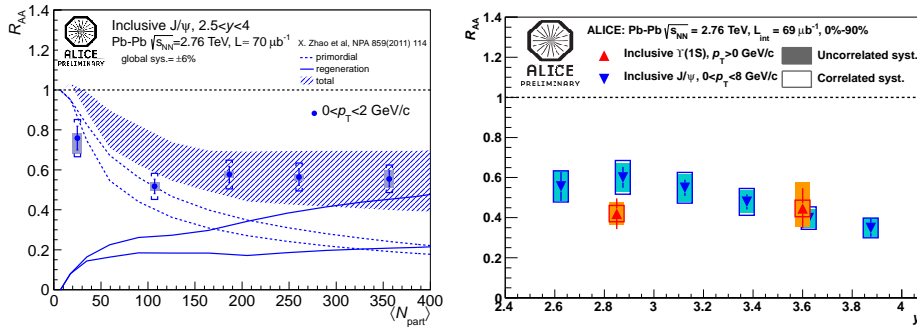


Fig. 4. – Left: J/ψ nuclear modification factor *vs.* number of participants in Pb-Pb collisions, compared to transport model predictions. Right: J/ψ and $\Upsilon(1S)$ nuclear modification factor in Pb-Pb collisions, as a function of rapidity.

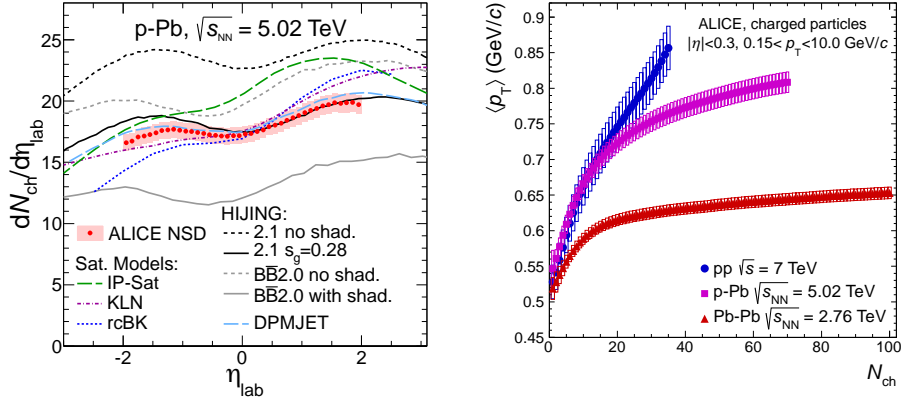


Fig. 5. – Left: pseudorapidity distribution of charged particles in p-Pb collisions, compared to saturation and pQCD models. Right: average transverse momentum of charged particles *vs.* charged multiplicity for pp, p-Pb and Pb-Pb collisions.

The suppression of quarkonium production by colour screening was one of the first signatures proposed for the QGP [11]. Charmonium regeneration due to the recombination of initially uncorrelated c and \bar{c} quarks may also become relevant at LHC energies [12]. Figure 4 shows the J/ψ R_{AA} as a function of centrality (number of participants, left) and rapidity (right). The observed suppression is independent of centrality at large number of participants, an effect compatible with a scenario where a large fraction of the J/ψ yield comes from regeneration. The nuclear modification factor for $\Upsilon(1S)$ was also measured, as shown in fig. 4, right.

3. – Highlights from p-Pb collisions

The charged particle pseudorapidity (η_{lab}) density distribution in p-Pb collisions was measured [13] and compared with available models (fig. 5, left). It was found that, while all models reproduce the data within 20%, saturation models seem to predict too steep a dependence on η_{lab} . pQCD-based models are in better agreement with the measured slope. The average transverse momentum as a function of the event charged particle multiplicity N_{ch} has been measured for p-Pb collisions and compared to pp and Pb-Pb collisions [14] (fig. 5, right). The average p_T in p-Pb collisions follows the one of pp collisions up to $N_{ch} = 14$, and shows a much stronger increase with respect to Pb-Pb collisions. The difference between pp and p-Pb at large multiplicities is not explained by the difference in collision energy alone. A superposition of independent pp collisions (Glauber approach), with the measured p_T from pp collisions, underestimates the average p_T in p-Pb collisions. This may signal the presence of collective final state effects, color reconnection between hadronizing strings, or coherent effects between strings formed in different nucleon-nucleon collisions. Di-hadron correlation results in p-Pb collisions have recently been obtained [15]: going from low-to-high multiplicity collisions, a near-side ridge becomes evident. In order to quantify the change from low-to-high multiplicity, the per-trigger yield for the low-multiplicity class (60–100%) is subtracted from that of the high-multiplicity class (0–20%) (see fig. 6). The near-side ridge is accompanied by a similar structure on the away side, not predicted by the HIJING event generator.

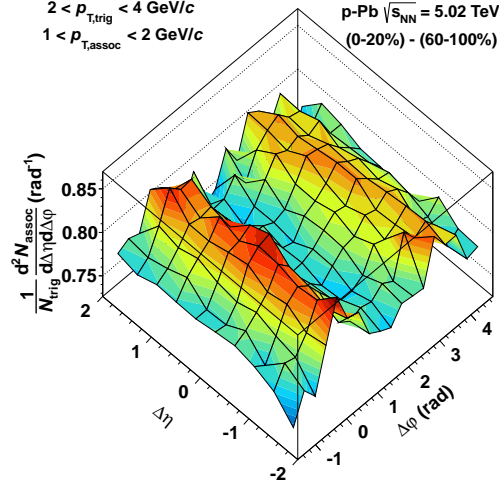


Fig. 6. – Associated yield per trigger particle for pairs of charged particles in p-Pb collisions for the 0–20% multiplicity class, after subtraction of the associated yield obtained in the 60–100% event class.

4. – Highlights from pp collisions

The inelastic (fig. 7, left), single diffractive (fig. 7, right) and double diffractive cross sections were measured in pp collisions at $\sqrt{s} = 2.76$ and 7 TeV [16], compared to other measurements at the LHC and to predictions from current models and found to be consistent with all of these, within the present uncertainties. The cross sections and transverse momentum distributions of D mesons (fig. 8, left) and of electrons and muons from heavy-flavour decays have been measured in pp collisions at $\sqrt{s} = 2.76$ and 7 TeV [17].

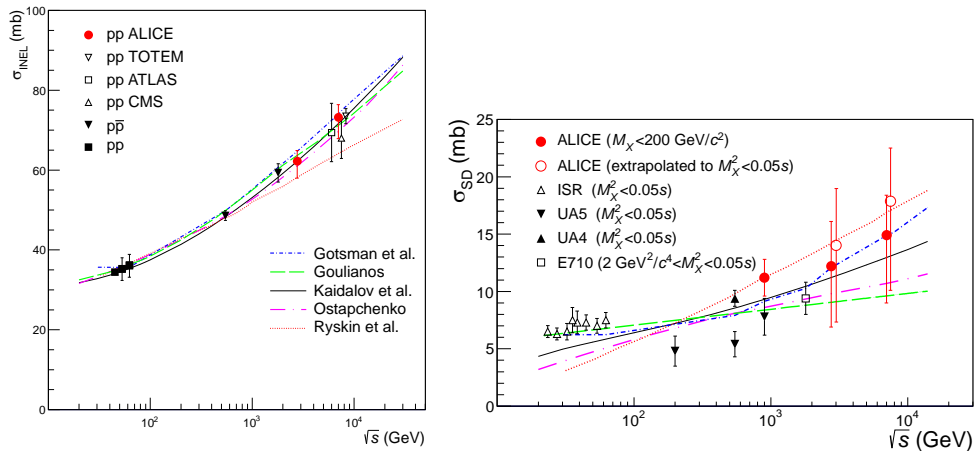


Fig. 7. – Inelastic (left) and single diffractive (right) cross sections in pp collisions at $\sqrt{s} = 2.76$ and 7 TeV, compared to measurements by other experiments and to models.

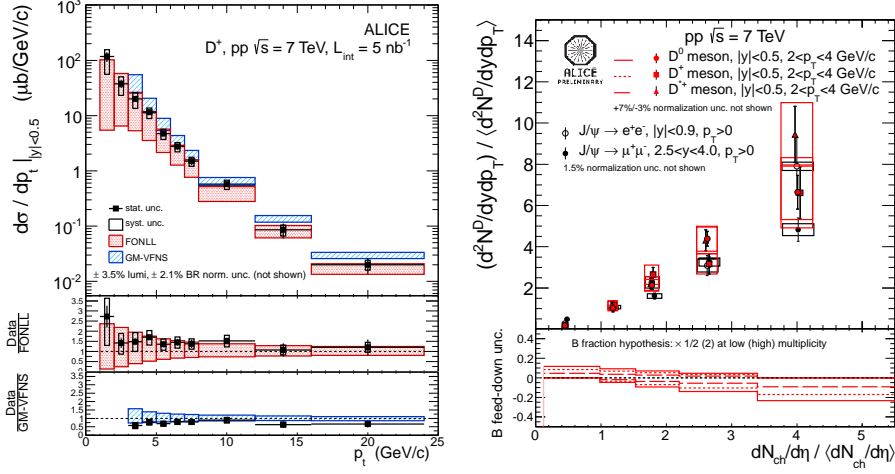


Fig. 8. – Left: D^+ meson cross section as a function of p_T in pp collisions at $\sqrt{s} = 7$ TeV, compared to pQCD calculations. Right: J/ψ and D meson yield as a function of the charged particle multiplicity density. Both the yield and the multiplicity density are normalized to their average values in minimum bias pp collisions.

Perturbative QCD calculations in the FONLL [18] scheme were found to be in agreement with the measured spectra. The D meson yields were also measured as a function of the event multiplicity (fig. 8, right) and an approximately linear increase of the yield with multiplicity was observed. A similar behaviour is observed for J/ψ [19].

REFERENCES

- [1] AAMODT K. *et al.* (ALICE COLLABORATION), *JINST*, **3** (2008) S08002.
- [2] EVANS L. *et al.*, *JINST*, **3** (2008) S08001.
- [3] KARSCH F., BNL-NT-06/2 (hep-lat/0601013).
- [4] AAMODT K. *et al.* (ALICE COLLABORATION), *Phys. Lett. B*, **696** (2011) 328.
- [5] AAMODT K. *et al.* (ALICE COLLABORATION), *Phys. Rev. Lett.*, **105** (2010) 252301; **106** (2011) 032301.
- [6] ABELEV B. *et al.* (ALICE COLLABORATION), *Phys. Rev. Lett.*, **109** (2012) 252301.
- [7] SCHNEDERMANN E. *et al.*, *Phys. Rev. C*, **48** (1993) 2462.
- [8] AAMODT K. *et al.* (ALICE COLLABORATION), *Phys. Rev. Lett.*, **105** (2010) 252302.
- [9] HEINZ U. W. *et al.*, *AIP Conf. Proc.*, **1441** (2012) 766; *Phys. Rev. C*, **84** (2011) 044903.
- [10] ABELEV B. *et al.* (ALICE COLLABORATION), *Phys. Lett. B*, **719** (2013) 18.
- [11] MATSUI T. and SATZ H., *Phys. Lett. B*, **178** (1986) 416.
- [12] BRAUN-MUNZINGER P. and STACHEL J., *Phys. Lett. B*, **490** (2000) 196.
- [13] ABELEV B. *et al.* (ALICE COLLABORATION), *Phys. Rev. Lett.*, **110** (2013) 032301.
- [14] ABELEV B. *et al.* (ALICE COLLABORATION), *Phys. Lett. B*, **727** (2013) 371.
- [15] ABELEV B. *et al.* (ALICE COLLABORATION), *Phys. Lett. B*, **719** (2013) 29.
- [16] ABELEV B. *et al.* (ALICE COLLABORATION), *Eur. Phys. J. C*, **73** (2013) 2456.
- [17] ABELEV B. *et al.* (ALICE COLLABORATION), *JHEP*, **01** (2012) 128; **07** (2012) 191; *Phys. Lett. B*, **708** (2012) 265; *Phys. Rev. Lett.*, **109** (2012) 112301; *Phys. Rev. D*, **86** (2012) 112007.
- [18] CACCIARI M. *et al.*, *JHEP*, **10** (2012) 137.
- [19] ABELEV B. *et al.* (ALICE COLLABORATION), *Phys. Lett. B*, **712** (2012) 165.